Ab initio investigation of the native defects in diamond and self-diffusion

S. J. Breuer and P. R. Briddon

Department of Physics, The University of Newcastle upon Tyne, Newcastle upon Tyne NE1 7RU, United Kingdom

Local-density-functional pseudopotential theory is used to investigate native defects in diamond, their structure, electronic, vibrational, and diffusive properties. We find the only truly stable structure for an interstitial atom to be the $\langle 100 \rangle$ split interstitial defect. This conclusion holds in the neutral, -1, $+1$, and $+2$ charge states. We analyze the multiplet structure of this defect, finding $^1B_1$ to be the lowest in energy. However, a Jahn-Teller distortion is also possible in all but the $+2$ charge state, giving considerable reductions in energy (0.6 eV for the neutral case). The tetrahedral, hexagonal, bond-centered, and $\langle 110 \rangle$ split interstitial structures are shown to be unstable. An upper bound for the energy barrier to the motion of the $\langle 100 \rangle$ split interstitial is found to be 1.7 eV. This is lower than that of vacancy diffusion although movement of interstitial atoms is usually ignored in considering self-diffusion. For the vacancy in diamond, we find that the surrounding four atoms relax *outwards* by 0.2 Å in both the neutral and negative charge states. The neutral vacancy undergoes a Jahn-Teller distortion with an energy gain of 0.36 eV. This effect is known to be dynamic at room temperature. For the negative vacancy we obtain $^4A_2$ as the ground state and obtain the transition energy to $^4T_1$ to be 3.3 eV, in good agreement with the observed ND1 band at 3.149 eV. Energies of other multiplets are estimated. We find the migration energies of the neutral and negative vacancies to be 2.8 and 3.4 eV, respectively. Finally, we calculate the formation energy for a vacancy-$\langle 100 \rangle$ split interstitial pair to be 20 eV.

I. INTRODUCTION

Diamond has come to be recognized over recent years as a technologically very important material. Currently, research continues into the important area of the growth of thin films by various processes. The material thus produced has a wealth of possible uses and much has been published on present and possible future applications. The process of diffusion in the bulk material or within the manufactured thin films is still not properly understood. There has been work published over the past two decades on self-diffusion and native defects in diamond, however this is just a fraction of that published on the same processes in silicon. The aim of this paper is to give a comprehensive analysis of all of the important native point defects in diamond and their migration through the perfect diamond lattice, using state of the art computational techniques, which have no experimental input. The work is compared with previous results found using theoretical techniques of various levels of sophistication and experimental findings.

There are still questions as to the stability of the various possible self-interstitial configurations of atoms. Five possible interstitial defects in tetrahedral semiconductors have been proposed. These are the tetrahedral, hexagonal, bond-centered, $\langle 100 \rangle$ and $\langle 110 \rangle$ split interstitials, as shown in Figs. 1(a)–1(d). In the past, different conclusions have been reached, using various techniques, as to which is the most stable of these structures in group IV semiconductors. The first investigations on diamond were carried out using semiempirical methods with experimental parameter input. Weigel et al.[1] used extended Hückel theory and found that the hexagonal and

tetrahedral site interstitials were unstable and that the $\langle 100 \rangle$ split interstitial and bond-centered defects were interchangably the most stable, depending on the charge state. Mainwood et al.[2] used a complete neglect of differential overlap (CNDO) method, producing the result that the $\langle 100 \rangle$ split interstitial had the lowest energy with the hexagonal site approximately 1.5 eV above. More recent work has used first-principles ab initio techniques, which are more sophisticated and do not have the severe approximations used by the older methods. To our knowledge, the first application of these methods was by Bernholc et al.[3] who modeled these defects using a supercell with the wave function and charge density expanded in terms of plane waves. They found that the bond-centered defect had the lowest formation energy for an interstitial atom in diamond with the $\langle 100 \rangle$ split interstitial 0.9 eV above. The supercell used contained only 16 atoms and so the very high defect concentration could have given rise to strong defect-defect interaction effects producing changes specific to that calculation. Chadi[4] has recently investigated interstitial atoms in silicon using a similar technique and found the $\langle 110 \rangle$ split interstitial to be the most energetically favorable.

The standard technique of irradiation of semiconductors by high-energy electrons causes extensive damage to the lattice and the formation of vacancies and interstitial defects. The vacancy in diamond has been much studied as experimental and theoretical evidence both point to it being the source of the GR1 band in its neutral charge state[5–8] and ND1 band in its negative charge state.[9,10] Experimental[11,12] and theoretical[13–16] estimations of the vacancy-interstitial pair formation energy have been made over many years. Also, more recently,
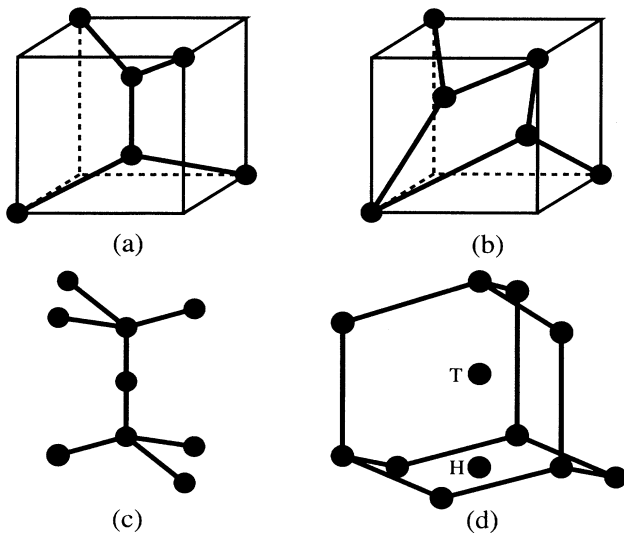
FIG. 1. Possible structures formed by the addition of an interstitial carbon atom to the diamond lattice. (a) The structure of the $\langle 100 \rangle$ split interstitial defect. The bond between the two central atoms is in the crystallographic $\langle 100 \rangle$ direction. (b) The structure of the $\langle 110 \rangle$ split interstitial defect. The two atoms within the cube are displaced from each other along the crystallographic $\langle 110 \rangle$ direction. (c) The structure of the bond-centered interstitial defect. (d) The ten atom cage in a tetrahedral lattice with the tetrahedral interstitial site (T) at the center and the hexagonal site (H) equidistant from the six atoms surrounding it.

Bernholc *et al.*[3] deduced the separate formation energies of the vacancy and various interstitial configurations.

The annealing of diamonds is a common process which directly involves and relies on the migration of carbon atoms in diamond. The theoretical calculation of diffusion barrier energies is complicated due to the number of possible paths the diffusing atoms can take. It can be difficult to be certain that the saddle point for diffusion has actually been found. This is especially the case with self-interstitials and is probably the reason for the lack of theoretical estimates of their migration energies. The self-diffusion energy was calculated by Bernholc *et al.*[3] for vacancy diffusion. The accurate experimental determination of diffusion energies is also a difficult task to carry out. The diffusion energy of the neutral vacancy in diamond has also recently been investigated experimentally[17,18] during annealing.

In Sec. II, we present details of the methods used in our calculations. In Secs. III–VI, we present our results for the self-interstitial structures, the vacancy, the formation energy of a vacancy-interstitial pair and the diffusion paths and energies of the self-interstitial and vacancy. Finally, in Sec. VII, we give our conclusions.

II. METHOD OF CALCULATION

The *ab initio* calculations performed here use the local-density approximation (or the local-spin-density approxi-

mation) to density functional theory, in which the Kohn-Sham[19] equations are solved self-consistently within a real space framework. The solid is approximated by using a large cluster of carbon atoms with hydrogen atoms on the surface of the cluster to tie up the dangling bonds. These bonds can otherwise give rise to levels in the band gap, which can interact with any defect levels present. The largest cluster used is the 304-atom cluster shown in Fig. 2, into which a vacancy-interstitial pair is put (Sec. V). The pseudopotential of Bachelet *et al.*[20] was used for the carbon atoms and the bare Coulombic potential was used for the hydrogen atoms.

Various different clusters were used in these calculations. Several factors are taken into account in the choice of cluster. There must be appropriate sites for the particular defects to be studied, usually near the center of the cluster and always at an acceptable distance from the surface. The symmetry of the cluster, before the defect is introduced, is preferentially as high as possible. The cluster should be large enough to allow sufficient relaxation around the defect. The advantage of using clusters of the size that we have used is that the terminating hydrogen atoms are generally at fourth-nearest-neighbor distances from each of the defect sites. The reasoning behind this approach is that the distance between the surface and defect site is sufficient to ensure that the structure of the defect is not significantly perturbed by the surface of the cluster, so that we are effectively modeling one defect in an infinite lattice. In an alternative approach, in which
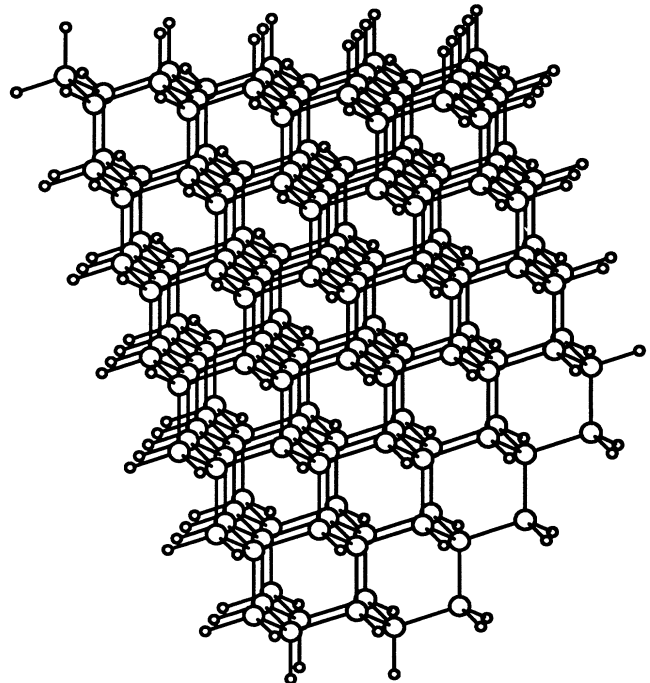
FIG. 2. The cluster $C_{190}H_{114}$ used in the calculations. The hydrogens are the atoms with the smaller radii, at the surface of the cluster.

the defect is placed at the center of a large unit cell (a supercell), the defect-defect distance is an analogous consideration. Our defect-surface separation corresponds to that obtained with a point defect placed in a 64 atom supercell. In that case, the defect-defect separation is effectively eight bond lengths, but the distance from any defect to the point midway between it and a neighboring defect is four bond lengths, the same distance that we generally have between a defect and the surface of the cluster. The carbon-carbon bond length in the perfect diamond clusters (before any structural relaxation) was set to 1.54 Å.

The total energy of the clusters was minimized with respect to the positions of the atoms to obtain the equilibrium structure in each case. The choice of which atoms were allowed to move depended on the defect and cluster size, and details of this are given as each cluster is introduced in the paper.

The charge density and wave function of the cluster are fitted to a set of localized Gaussian-type orbitals centered on the positions of the atoms. These orbitals are made s and p type by a multiplicative factor. For each carbon atom, 16 different Gaussians (s, p_x, p_y, and p_z type functions with four different exponents) were used to expand the wave function of the 2s and 2p states, and Gaussians with four different exponents were used to fit the charge density. This full basis for the carbon atoms is used on the innermost atoms including and surrounding the defect. The carbon atoms closest to the edge of the cluster had a contracted basis in which four orbitals were used to describe the wave function (with character s, p_x, p_y, and p_z), each of which is a fixed linear combination of four Gaussians. For each of the terminating hydrogen atoms, Gaussians with three different exponents were used to fit the charge density and a linear combination of s-type orbitals with two exponents and a linear combination of p_x, p_y, and p_z type orbitals, each with two exponents were used to fit the wave function. The actual numbers of carbon atoms in each basis is given with the details of each particular cluster. In diamond the use of localized Gaussian orbitals avoids a problem usually encountered by an alternative approach using plane wave expansions in supercells of a very high cutoff frequency. This is due to the hardness of the pseudopotential required to model carbon atoms accurately.

It should be stressed that there is no empirical data input, only the atomic numbers of the atoms and their positions are required. This approach has been successfully used in previous calculations of, for example, the phonon spectrum of diamond[21] and the structure and vibrational properties of various nitrogen containing defects in diamond.[22,23] In particular, the lattice constant and Raman frequency of diamond are in excellent agreement with experiment.

Each structure was relaxed until the energy had converged to 10^{-5} a.u. Each defect was investigated in the charge states considered important or appropriate. The details of the method are essentially the same as that described in detail in a previous paper[21] with some modifications, which will be described in a forthcoming paper.

III. SELF-INTERSTITIAL DEFECTS

All calculations for self-interstitials were carried out in the -1, 0, $+1$, and $+2$ charge states. The cluster used for comparing the energy of the relaxed interstitial defects has 163 atoms ($C_{93}H_{70}$) and C_{3v} symmetry. This is suitable as it contains a substitutional site and tetrahedral, hexagonal, and bond-centered interstitial sites, which are all distant from the surface of the cluster, making it suitable for the comparison of the energies of the different defects.

With the addition of another carbon atom to form the interstitial defects, the innermost 30 carbon atoms were in full basis and these same atoms were allowed to move to optimize the structure. This cluster contains sites for each defect within two atomic spacings of the center of the cluster.

When we are studying one specific defect, such as a split interstitial, it is not necessary to use such a large cluster as we no longer need to have a variety of high symmetry interstitial sites, which are all distant from the surface of the cluster. Therefore a second cluster was used containing 131 atoms ($C_{71}H_{60}$). This cluster has tetrahedral symmetry about a central substitutional site, and only the presence of the defect lowers this. With the addition of the interstitial atom, 18 atoms were in full basis and all the carbon atoms were allowed to move.

A. The $\langle 100 \rangle$ split interstitial

The central carbon atom in the 131 atom cluster was replaced by two carbon atoms displaced along the [100] and [$\bar{1}$00] directions from the lattice site by roughly half a carbon-carbon bond length. This starting structure has D_{2d} symmetry. Two one-electron energy levels appeared towards the top of the band gap. The wave functions of these were basically p orbitals centered on the two carbon atoms forming the interstitial pair (atoms C and D in Fig. 3) pointing out of the planes containing their three neighbors. In general, one would expect bonding and antibonding combinations of these to be formed leading
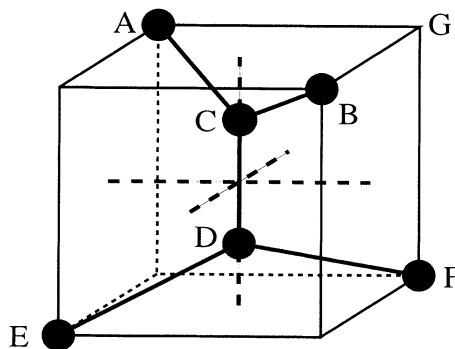
FIG. 3. The $\langle 100 \rangle$ split interstitial defect with the labeling of atoms used in the text. The dashed lines show the direction of the three perpendicular twofold rotation axes necessary for D_2 symmetry.

to a splitting of the two states, but this does not happen here as the two defect states are orthogonal and so do not mix.

In the neutral charge state, two electrons are placed into these two degenerate orbitals. The multiplet structure of this defect is, therefore, found from $e \otimes e$ evaluated in D_{2d} symmetry. This gives rise to $^1A_1$, $^3A_2$, $^1B_1$, and $^1B_2$. If we label the two one-electron states as ϕ_a and ϕ_b and the spin states as $\uparrow$ and $\downarrow$, the multiplets are

$$^1A_1 : [\phi_a(1)\phi_a(2) + \phi_b(1)\phi_b(2)][\uparrow\downarrow - \downarrow\uparrow],$$

$$^1B_2 : [\phi_a(1)\phi_a(2) - \phi_b(1)\phi_b(2)][\uparrow\downarrow + \downarrow\uparrow],$$

$$^1B_1 : [\phi_a(1)\phi_b(2) + \phi_b(1)\phi_a(2)][\uparrow\downarrow - \downarrow\uparrow],$$

$$^3A_2 : [\phi_a(1)\phi_b(2) - \phi_b(1)\phi_a(2)] \left\{ \begin{array}{c} [\uparrow\uparrow] \\ [\uparrow\downarrow + \downarrow\uparrow] \\ [\downarrow\downarrow] \end{array} \right\}.$$

Density-functional theory was originally presented as a method for determining ground state properties. However, a study of methods by which approximate multiplet splittings can be obtained from density-functional theory has been carried out.[24] There it is shown that if a one-electron configuration contributes to only a single multiplet state, then the local-density approximation to the energy of that configuration is a reasonable estimate of the energy of the multiplet. That is clearly the case, for example, for the one-electron configuration in which electrons are placed with parallel spins into each of the two states, i.e., $|a \uparrow\rangle|b \uparrow\rangle$. The energy of this is an estimate of that of the $^3A_2$ state. We first used this configuration in the 132 atom cluster described above and relaxed the central atoms to get the atomic structure and energy of the $S = 1$ state. With this atomic structure, the approximate energies of the different multiplets can then be found by following von Barth.[24] The energy of the mixed state $|a \uparrow\rangle|b \downarrow\rangle$ is the average of the $^1B_1$ and $^3A_2$ multiplets so that the energy of $^1B_1$ can also be determined. Similarly the energy of $|a \uparrow\rangle|a \downarrow\rangle$ is the average of the energies of $^1A_1$ and $^1B_2$. It is not possible to find the energies of these separately, as we do not have any additional distinct one-electron configurations (i.e., we have more multiplets than distinct configurations). As a result, we have an underdetermined set of equations for the evaluation of the multiplet energies. This is the opposite problem to that encountered by von Barth,[24] who had an overdetermined set of equations. We find the energy of $^1B_1$ to be 0.55 eV lower than $^3A_2$, whereas the average of the energies of $^1A_1$ and $^1B_2$ lies 1 eV higher than $^3A_2$. In this case, our calculations suggest that Hund's rule fails to get the correct ground state.

For reference, we note that in the equilibrium structure for the $^3A_2$ electronic configuration, the e one-electron states fall 2.1 eV below the conduction band. This defect is, therefore, more likely to be seen in the positive charge states in type Ia and type II diamond, although its charge state is difficult to predict in type Ib diamond. The following discussion will therefore concentrate on both positive charge states and the single negative charge state. The doubly negatively charged state is almost certainly unstable even in type Ib diamond, as its level will move

above the Fermi level, which is fixed by the presence of $P1$ centers, and possibly even out of the band gap.

We now consider the possible Jahn-Teller distortion of this defect. Such a distortion is possible in the neutral or singly charged states in which the one-electron e states are partially occupied. In the doubly charged states, $+2$ or -2, the two one-electron states are either completely empty or completely occupied so that a Jahn-Teller distortion is not to be expected.

To investigate this, the two atoms of the $\langle 100\rangle$ split interstitial were made inequivalent and further relaxation was allowed. In only one of the charge states, the $+2$, did the defect recover D_{2d} symmetry. In the neutral, $+1$ and -1 charge states the final structure had D_2 symmetry. D_2 symmetry requires three perpendicular twofold rotation axes. These are shown in Fig. 3 and basically connect the centers of the opposite faces of the cube. D_{2d} symmetry also requires two vertical mirror planes. These are shown in Fig. 4 and cut the top and bottom faces of the cube in Fig. 3 diagonally. The structural relaxation, therefore, resulted in the loss of the two vertical mirror planes. The reason for this is that the two previously equivalent sides of the cube, AG and GB, in Fig. 3, become inequivalent. The sides of the cube in Fig. 3 for the relaxed neutral defect with D_2 symmetry had lengths $AG = 1.73$ Å, $GB = 1.98$ Å, and $GF = 2.19$ Å, with these distances varying by a maximum of 0.08 Å for the $+1$ and -1 charge states. These are to be compared with $AG = GB = 1.87$ Å and $GF = 2.19$ Å for the neutral structure with D_{2d} symmetry, with a maximum variation of 0.07 Å for the other charge states and $AG = GB = GF = 1.77$ Å for the perfect lattice. In all cases, the sides of the distorted cube remained perpendicular. The bond lengths corresponding to both the D_2 and D_{2d} symmetry structures are $CD = 1.26$ Å and $AC = BC = DE = DF = 1.40$ Å. It is interesting to note that the bond lengths are insensitive to the charge state, varying by at most 0.03 Å. There is a corresponding loss of electronic level degeneracy with the symmetry breaking structural relaxation, with the one-electron e state splitting into b_2 and b_3 levels with the lowest being doubly occupied. The same level splitting occurs for the $+1$ and -1 charge states. The difference in energy between the defect structures with D_{2d} and D_2 symmetry is the Jahn-Teller energy for the
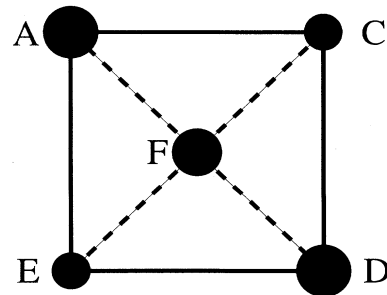
FIG. 4. The top face of the cube in Fig. 3 containing the $\langle 100\rangle$ split interstitial defect. The dashed lines show where the vertical mirror planes perpendicular to the top face cut that face.

system. This was calculated to be 0.6 eV for the neutral defect.

The vibrational properties of the neutral defect with D_2 symmetry were determined, including isotopic shifts. Initially, the second derivatives of energy with respect to displacements of the two atoms forming the interstitial together with their four neighbors were found, giving a 18×18 matrix of force constants. From this the dynamical matrix was constructed and the vibrational frequencies found, initially for all ^{12}C atoms. The highest frequency vibrational mode, which is associated with the stretching of the central carbon-carbon bond, is an A mode with frequency 2023 cm^{-1}. The next two highest-frequency modes are B modes associated with the motion of atoms C and D in Fig. 3 perpendicular to the [100] bond, but within the plane of their three neighbors. These had frequencies of 1590 and 1600 cm^{-1}. If one of the central ^{12}C atoms is replaced by a ^{13}C atom the modes become 1984 cm^{-1}, 1560 cm^{-1}, and 1595 cm^{-1}, respectively. If both of the central ^{12}C atoms are replaced by ^{13}C atoms the modes become 1944 cm^{-1}, 1557 cm^{-1}, and 1564 cm^{-1}, respectively. In fact, the A mode is infrared inactive, but the B modes are both active.

Finally, an atom was added to the 163 atom cluster described above and a $\langle 100 \rangle$ split interstitial was formed. The structure was relaxed and the energy found for each charge state. This enabled us to compare the energy between this and the remaining suggested structures for an interstitial atom investigated in the following sections.

B. Tetrahedral and hexagonal interstitials

The interstitial carbon atom was placed in turn at the tetrahedral and hexagonal interstitial sites in the 163 atom cluster. Initially, the structure was allowed to relax while the interstitial atom was constrained to remain at the appropriate symmetry site. This gave the best chance for the surrounding network to relax to accommodate and, thus, to stabilize the interstitial. However, after this initial relaxation, this constraint was removed and the interstitial atom was also allowed to move. This resulted in a substantial relaxation, with the interstitial atom migrating towards a neighboring host atom and forming a $\langle 100 \rangle$ split interstitial with that atom. This happened in all charge states. This contrasts with earlier empirical calculations in which energies for the interstitial atoms were reported.[2] This result gives very strong evidence for the global stability of the $\langle 100 \rangle$ structure as in these relaxations atoms moved considerable distances and yet no other structure was formed.

The multiplet structure of the neutral ideal (undistorted) tetrahedral interstitial is somewhat similar to that of the neutral vacancy to be considered in Sec. IV A. Three degenerate one-electron levels of symmetry t_2 appear in the band gap into which two electrons must be placed. This configuration is known to be unstable with respect to a Jahn-Teller distortion for the neutral vacancy, but in that case, the relaxation is limited by the constraints of the surrounding lattice. That is not the case here, and a much larger relaxation occurs leading to a $\langle 100 \rangle$ defect. In a similar way, the negatively charged interstitial can be compared to the negatively charged vacancy. For this defect, the undistorted $^4A_2$ state is the ground state as discussed in Sec. IV B. However, a distorted excited state with $S = \frac{1}{2}$ of the negative vacancy lies only 0.24 eV higher in energy than the $^4A_2$ state with distortion again being limited by the lattice. In the case of the negatively charged interstitial atom at the tetrahedral site, the lack of resistance to distortion again leads to the formation of a lower-energy $\langle 100 \rangle$ defect.

C. The bond-centered interstitial

The interstitial atom was put at the center of a carbon-carbon bond in the 163 atom cluster. The structure was relaxed with the atom forced to remain on the bond axis, thereby preserving C_{3v} symmetry. In each charge state the structure obtained had the bonds from the bond-centered atom to its two nearest neighbors at about 80% of the perfect diamond lattice bond length. The second- and third-nearest neighbors were displaced outwards in such a way that their bonds only differed in length from the perfect lattice value by at most 3%. For all the charge states, the energy of the bond-centered interstitial was found to be higher than that of the correspondingly charged $\langle 100 \rangle$ split interstitial (Table I). The increase of relative energy with the addition of electrons is consistent with one-electron energy levels high in the band gap. Without the enforced preservation of the initial symmetry the atom at the center of the bond moved to form a $\langle 100 \rangle$ split interstitial with one of the other two atoms in the structure in all charge states.

D. The $\langle 110 \rangle$ split interstitial

Recently, a most stable structure for split interstitials in silicon has been proposed by Chadi,[4] in which the split interstitial is oriented along $\langle 110 \rangle$ rather than $\langle 100 \rangle$. To study this structure in diamond, we replaced a central carbon atom in the 163 atom cluster by two atoms oriented along the $\langle 110 \rangle$ direction with a separation of 1.3 Å.

On relaxation of the structure the -1 and $+1$ charge

TABLE I. The energy of the bond-centered interstitial and $\langle 110 \rangle$ split interstitial defects relative to the $\langle 100 \rangle$ split interstitial defect for various charge states.

Charge state	-1	0	$+1$	$+2$
Relative energy of bond-centered interstitial (eV)	$+4.45$	$+4.05$	$+3.04$	$+2.32$
Relative energy of $\langle 110 \rangle$ split interstitial (eV)		$+2.53$		$+1.85$

states of the defect were found to be unstable with the atoms relaxing to form $\langle 100 \rangle$ split interstitials. Both the neutral and $+2$ charge states relaxed with the bond remaining in the $\langle 110 \rangle$ direction. However, these structures were found to be unstable when the atoms in the defect were given small symmetry breaking displacements of 0.025 Å and 0.005 Å, respectively. These displacements are considerably smaller than those associated with zero point motion of the defect, which is neglected in our calculation, and we can conclude that $\langle 110 \rangle$ split interstitials are not stable in diamond. In any case, if the structure was enforced, the energies of the neutral and $+2$ $\langle 110 \rangle$ split interstitials were higher than those of the $\langle 100 \rangle$ split interstitials (Table I). One possible reason for the stability of $\langle 100 \rangle$ defects is the preference in diamond for sp^2 bonding, which is in contrast to other elemental semiconductors such as silicon.

IV. THE VACANCY

The 131 atom cluster used in Sec. III A was again used for the vacancy. A carbon atom was removed from the cluster leaving an unrelaxed vacancy with tetrahedral symmetry. The central 16 carbon atoms were treated in full basis, and all 70 carbon atoms were allowed to move during structural optimization, unless otherwise specified. The symmetry dictates that the four carbon atoms surrounding the vacancy are initially equivalent. This ideal, unrelaxed vacancy has four dangling sp^3 hybrids pointing inwards, and in tetrahedral symmetry, these give rise to a one-electron state of a_1 symmetry, which falls just above the top of the valence band and three degenerate states of symmetry t_2, which occur deep in the band gap. All calculations for the vacancy were carried out for both the neutral and -1 charge states.

A. The neutral vacancy

In this charge state, four electrons must be placed into the one-electron states. In the ground state, two are placed into the a_1 state and two into the t_2 one-electron state giving the configuration $a_1^2 t_2^2$.

Initially, the three states were occupied equally with an effective occupancy of $\frac{2}{3}$ and the structure was allowed to relax, with the atoms moving to minimize the energy. With this rather artificial filling, tetrahedral symmetry was maintained and the four carbon atoms immediately surrounding the vacancy moved radially outwards by 0.2 Å. The sides of the cube in Fig. 5 had lengths $AE = BE = CE = 1.89$ Å after relaxation. The bonds from the first nearest neighbors of the vacancy to the second nearest neighbors and from the second to the third were shorter than those in the bulk by no more than 2%. This motion corresponds to an A mode relaxation. The relaxation is in the opposite direction to the results obtained by Mainwood[25] using a CNDO technique, who found that the atoms surrounding the vacancy relaxed inwards, but that a very weak metastable structure with outwards relaxation could be possible with a spe-
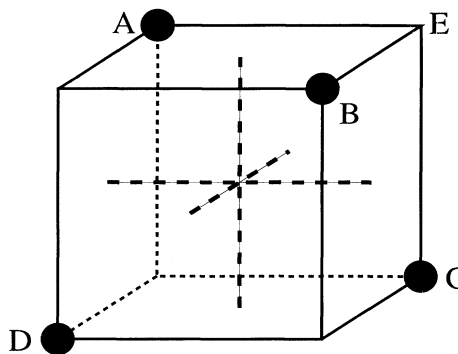
FIG. 5. The vacancy with labeling of atoms used in the text. The dashed lines show the direction of the three perpendicular twofold rotation axes necessary for D_2 symmetry.

cific choice of basis. To check our results, we have frozen the four atoms surrounding the vacancy at various radial displacements from their positions in the perfect lattice, and allowed all the remaining 66 carbon atoms to relax. The energy plotted as a function of the fixed displacements of the four neighbors of the vacancy is shown in Fig. 6, and shows no evidence for inwards motion. The outwards relaxation is understandable from a chemical bonding point of view. It leads to the atoms surrounding the vacancy moving more into the plane of their three nearest neighbors, and the bonding becoming more like sp^2 than sp^3, with the former being preferred.

Clearly, the one-electron configuration t_2^2 is unstable with respect to a Jahn-Teller distortion, and, in fact, we find this to be the case with one of the cubic axes becoming inequivalent to the other two. The symmetry changes from tetrahedral to D_{2d} corresponding to an E mode relaxation. With reference to Fig. 5, the sides of
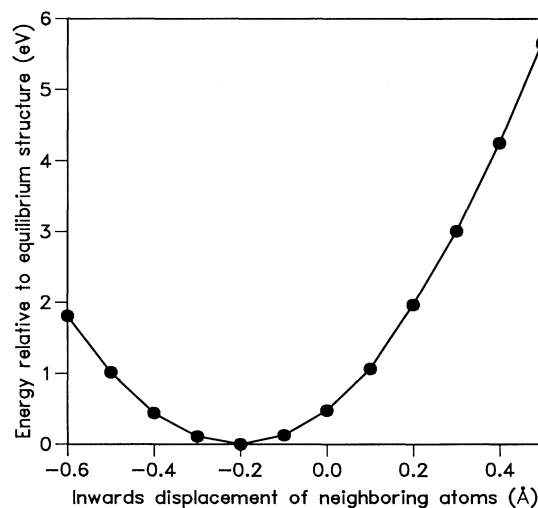
FIG. 6. The energy of a relaxed neutral vacancy in eV as a function of the fixed inward radial displacement of the four surrounding atoms relative to their position in the perfect lattice. The zero of energy is for the equilibrium vacancy structure.

the cube for the relaxed neutral defect with D_{2d} symmetry have lengths $AE = BE = 1.78$ Å and $CE = 2.00$ Å. The effect of this distortion is to split the t_2 one-electron states into a doubly occupied a state and an unoccupied e state. The Jahn-Teller energy associated with the relaxation of the neutral vacancy was found to be 0.36 eV, somewhat larger than an approximate experimental value of 0.2 eV.[17]

This Jahn-Teller relaxation is similar to the situation observed in silicon, in which the static distortion can be demonstrated experimentally. However, in diamond, optical experiments carried out at room temperature show the Jahn-Teller effect to be dynamic, so that the optical absorption is analyzed in terms of multiplets of a defect with effective T_d symmetry. The multiplet structure of this effectively tetrahedral center has been most effectively treated using empirical methods following Coulson and Kearsely[26] and work on related models is continuing.[27] It is established that the ground state is ^1E with a vibronic state only just higher in energy by a few meV.[28] The best known signature of this defect is the GR1 band with a zero phonon line at 1.673 eV. This is believed to be associated with a transition from the ground ^1E state to $^1T_2$. Unfortunately, it is not possible to determine the energy of the ground state ^1E using density-functional theory as only a weighed value of the energies of $^1A_1$ and ^1E can be found. We will not pursue this calculation further here.

B. The negative vacancy

For the negative vacancy, five electrons need to be placed into the one-electron states. The lowest-energy states of this defect will correspond to the one-electron configuration $a_1^2 t_2^3$.

It is known experimentally[10] that the ground state of the negative vacancy is the many body state $^4A_2$ to which only a single one-electron configuration contributes, the one in which electrons are placed into each of the degenerate t_2 states with parallel spins. For this electronic configuration we find on relaxation that each of the four atoms surrounding the vacancy moves radially outwards by 0.2 Å. The sides of the cube in Fig. 5 then have lengths $AE = BE = CE = 1.89$ Å. This is almost identical to the case of the neutral vacancy in which each of the t_2 states is equally occupied. For this electronic state and structure, we find that the t_2 states lie approximately 3.9 eV above the top of the valence band, still well below the conduction band which is 2.5 eV higher in energy.

It is accepted that the ND1 optical band seen at 3.149 eV is associated with a transition from $^4A_2$ to $^4T_1$. In the noninteracting limit, only a single configuration contributes to $^4T_1$, namely, $a_1 t_2^4$ in which the electrons are placed in the orbitals as $\xi_\uparrow \xi_\downarrow \eta_\uparrow \zeta_\uparrow$, where ξ, η, and ζ label the three one-electron states of symmetry t_2. The energy of this multiplet can be evaluated using density-functional theory and we calculated the energy of the ND1 band to be 3.3 eV, in excellent agreement with experiment. In evaluating this transition energy, the positions of the nuclei were kept fixed in the equilibrium structure of the $^4A_2$ ground state in accordance with the Franck-Condon principle.

The energies of other multiplets can also be obtained approximately using density-functional theory. In particular, we obtain the ^2E state to be 0.3 eV above the $^4A_2$ ground state and the average of the $^2T_1$ and $^2T_2$ multiplets to be at 1.6 eV above $^4A_2$. This placing of ^2E is considerably lower than in empirical methods[29] in which it is placed between 1.4 eV and 1.9 eV above $^4A_2$, depending on the choice of parameters. Our placing of the average of $^2T_1$ and $^2T_2$ multiplets is in reasonable agreement with the empirical calculations. As optical transitions between $^4A_2$ and these are forbidden, experiment has not yet established their ordering or positioning.

Finally, in this section, we consider possible Jahn-Teller distortions of this defect. The structural symmetry of the vacancy was first constrained to be that of a subgroup of T_d. C_{2v}, C_{3v}, D_2, and D_{2d} were all considered as possible distortions. Structural relaxations using spin polarization were then carried out with the appropriate electronic occupancies for each case. The three electrons originally placed into the three degenerate t_2 one-electron levels in the T_d symmetry vacancy were placed into the one-electron levels which arose in each structure from the splitting of the t_2 levels. This procedure was carried out for all plausible nonequivalent cases. For three of the atomic symmetries it was necessary to consider only one possible electronic configuration. These were $e^2(\uparrow)a_1(\downarrow)$ for the C_{3v} symmetry structure, $b_1(\uparrow)b_2(\uparrow)b_3(\downarrow)$ for the D_2 symmetry structure, and $e^2(\uparrow)b_2(\downarrow)$ for the D_{2d} symmetry structure. For the C_{2v} symmetry structure, it was necessary to consider five possible electronic configurations; $b_1(\uparrow)a_1(\uparrow)b_1(\downarrow)$, $b_1(\uparrow)a_1(\uparrow)b_2(\downarrow)$, $b_1(\uparrow)a_1(\uparrow)a_1(\downarrow)$, $b_1(\uparrow)b_2(\uparrow)a_1(\downarrow)$, and $b_1(\uparrow)b_2(\uparrow)b_1(\downarrow)$. The configuration $b_1(\uparrow)a_1(\uparrow)b_2(\downarrow)$ gave the relaxed C_{2v} symmetry structure with the lowest energy. Using this total energy for the C_{2v} case, we found that the energies of the relaxed distorted structures above the ground state T_d symmetry structure were 0.24 eV for the C_{3v} case, 0.4 eV for the C_{2v} case, 0.75 eV for the D_2 case, and 0.89 eV for the D_{2d} case. Therefore, the $S = \frac{1}{2}$ Jahn-Teller distorted state has a higher energy than the $^4A_2$ state. This conclusion is supported by experiment in which it is known that the ground state of the negative vacancy has $S = \frac{3}{2}$. Thus, it is seen that in this case Hund's rule does, in fact, predict the correct ground state.

It is interesting to note that the energy splitting between the ground $S = \frac{3}{2}$ and excited $S = \frac{1}{2}$ states of the defect will, in fact, be given rigorously by density-functional theory. This is because both of these states are the ground-electronic states of their respective structures (as defined by the positions of the atomic nuclei). The fact that the undistorted $^4A_2$ state has a lower energy than the Jahn-Teller distorted state again marks diamond out as different from silicon in that many-body correlation effects dominate the energy gain from the Jahn-Teller distortion in determining the ground state and, thus, provides a more demanding challenge to theory. In silicon, it is generally accepted[30] that the ground state of the negative vacancy has C_{2v} symmetry, with

electrons being placed in the states $a_1(\uparrow)$, $b_1(\uparrow)$, and $a_1(\downarrow)$. In particular, a recent local-density calculation, which assumed this structure, has been able to reproduce the experimentally observed hyperfine couplings.[31]

V. THE VACANCY-⟨100⟩ INTERSTITIAL PAIR

Finally, in considering the static properties of native defects, we estimated the energy required to form a vacancy-⟨100⟩ split interstitial pair. A 304 atom cluster ($C_{190}H_{114}$) (Fig. 2) was used with the innermost 37 carbon atoms in full basis. Using this cluster, it was possible to create a vacancy and split interstitial with both at fourth neighbor distance from the surface of the cluster but with the defects at sixth neighbor distance from each other.

The total energy of a perfect 304 atom cluster (i.e., with the atoms placed in the diamond structure) was first determined. Then, the total energy of the 304 atom cluster, this time containing a relaxed vacancy and ⟨100⟩ split interstitial was found. The difference between these total energies was 20 eV and provides an estimate of the energy required to form a relaxed vacancy-⟨100⟩ split interstitial pair at a separation such that the relaxation of the atoms surrounding each defect does not affect the other defect. This can be compared with the sum of the formation energies of the neutral vacancy and ⟨100⟩ split interstitial calculated theoretically by Bernholc *et al.*[3] to be 23.9 eV. A possible reason why we obtain a smaller value is that in our cluster, both defects were not created in the neutral charge state — as charge was able to transfer between them. That was not the case in Bernholc's calculation in which the formation energies were calculated separately. A crude experimental estimate is 35 ± 5 eV[11].

VI. DIFFUSION PATHS

A. Self interstitial diffusion

As the ⟨100⟩ split interstitial was found to be the only stable structure for an interstitial carbon atom, we have only investigated the diffusion of this model of the interstitial. A 176 atom cluster ($C_{98}H_{78}$) with D_{3d} symmetry was used for this purpose. With the addition of the interstitial atom, the innermost 27 atoms were in full basis and the innermost 45 atoms were allowed to move to optimize the energy at each stage. The cluster is centered on the midpoint of a carbon-carbon bond and so has two equivalent substitutional sites close to the center of the cluster. Figures 7 and 8 show the important atoms involved in the diffusion path analysis and the atomic sites are labeled. The atoms are in the perfect tetrahedral diamond lattice positions. The center of the cluster and the origin of the Cartesian coordinate axes is at point E. The bond AF is along the D_{3d} symmetry axis of the cluster.
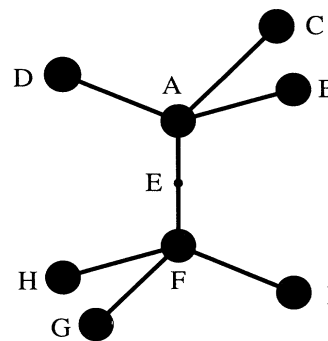
FIG. 7. The atoms involved in the investigation of diffusion, with labeling as referred to in the text.

The approximate path of diffusion for this defect is not easy to decide upon. Clearly, the lowest energy diffusion path will be the one which involves the stretching or breaking of the smallest number of bonds. We consider this to be the path in which an atom passes through a bridge bonded structure. In this model, an initial [100]-oriented defect becomes oriented along either [010] or [001] after diffusion. We first added a single carbon atom to the 176 atom cluster, to create the [100]- and [010]-oriented defects, at sites A and F, respectively, in Fig. 7. Our cluster was arranged such that the bond AF was along the [111] direction. These structures were relaxed to provide the end point coordinates for diffusion.

The vector of displacements connecting the positions of the equivalent atoms in the two relaxed end-point structures were determined, i.e., $\mathbf{v}_i = \mathbf{R}_i^A - \mathbf{R}_i^F$, where $\mathbf{R}_i^A$ is the position of atom i when the [100] interstitial is at site A, and $\mathbf{R}_i^F$ is the position of atom i when the [010] split interstitial is at site F. Then all the atoms were moved the same fraction, α, along this vector giving the positions of the atoms at an intermediate stage in the diffusion process. This was carried out for a series of values of α ranging between 0 and 0.5. For each of these structures the 45 atoms immediately surrounding and including the defect were allowed to move to optimize the energy, but subject to the constraint that the vector of further displacements should be perpendicular to the vector $\mathbf{v}_i$ connecting the end points defined above. This defines an energy profile for the diffusion process as a function of α and the maximum value of this gives the energy barrier to diffusion.
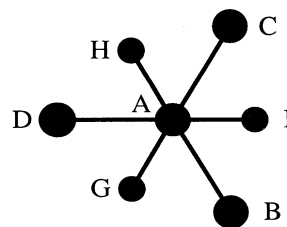
FIG. 8. The atoms involved in the investigation of diffusion (Fig. 7) as viewed along [111].

We find that the saddle point occurs for $\alpha = 0.5$. At this point the diffusing atom is displaced from point E (Fig. 7) by (0.00, −0.43, 0.43) Å. The atoms originally at the sites A and F are displaced from the perfect positions by (0.12, −0.03, −0.44) Å and (−0.12, 0.03, 0.44) Å, respectively. The atoms originally at sites B, C, D, G, H, and I are displaced from the perfect positions by no more than 0.2 Å. The barrier for diffusion of the neutral ⟨100⟩ split interstitial was hence found to be 1.7 eV along the path investigated. We believe this to be the most reasonable path, but cannot rule out a lower energy mechanism.

There have not been many determinations of the energetics of self-interstitial diffusion previously. One of the findings of Sec. III A was that the ⟨100⟩ split interstitial with D_2 symmetry has a highest-frequency vibrational mode that is infrared inactive. In recent experimental investigations[17,18] of the self-diffusion energetics, the characteristic infrared active modes of particular defects were used to deduce the diffusing defect. None have yet been linked to the ⟨100⟩ split interstitial, which could be used to measure changes in the concentration of the defect if it diffused to a site where it transformed into another defect. Such trapping points as dislocations or interstitial aggregations have been proposed in the past as well as possible straightforward recombination with a vacancy. There is an unexplained fast process, which took place over a time scale much less than that over which the measurements were taken in the experimental work mentioned.[17,18] Bernholc et al.[3] dismissed the importance of the self-interstitial in self-diffusion due to it having a larger formation energy than the vacancy. However, the practice of irradiating diamonds with high energy electrons must produce equal concentrations of vacancies and interstitials. It is not known which would be the most effective trapping centers for self-interstitial diffusion and the importance of the diffusion of this defect could depend on this.

B. Vacancy diffusion

An 86 atom cluster ($C_{44}H_{42}$) with C_{3v} symmetry was used for the vacancy diffusion calculations. With the removal of a carbon atom to form the vacancy, the innermost 25 atoms were in full basis and all the carbon atoms were allowed to move. The cluster is centered on the midpoint of a carbon-carbon bond and so has two equivalent substitutional sites near to the center of the cluster. The vacancy can, therefore, be centered at one of the sites and the diffusion path to the other site determined. All calculations on vacancy diffusion were carried out for both the neutral and −1 charge states. Referring to Fig. 7, one of the two equivalent atoms A and F in the perfect 86 atom cluster was removed and the 43 innermost atoms were allowed to move so that the total energy of the equilibrium structure was found. This produced the end-point structure for vacancy diffusion.

The approach first used to find the energy barrier for the diffusion of the vacancy was that used by Bernholc et al.[3] The assumption made in this case is that the path of

diffusion involves an atom moving from a site neighboring the vacancy, in a straight line $\mathbf{AF}$ to the vacancy site while all the surrounding atoms relax at each step. The saddle point was assumed to be midway between the substitutional sites. To investigate this, atoms A and F were replaced by one atom at point E. This atom was fixed at that position and the surrounding 42 atoms were relaxed to find the total energy of the saddle point of vacancy diffusion in this approach. The outwards relaxation of the surrounding atoms retained the D_{3d} symmetry. The value that was obtained was 3.3 eV using this approach for the neutral vacancy and 2.9 eV for the negatively charged vacancy.

A more complete investigation of the diffusion path was then carried out to find whether a lower energy saddle point existed. In this study, the two central atoms, A and F, were again replaced by a single atom, which was placed at a point a certain fraction between the sites A and F, $\alpha \mathbf{R}_A + (1 - \alpha)\mathbf{R}_F$, say where $0 \le \alpha \le 1$. This atom was then given a symmetry-breaking displacement in the plane perpendicular to the vector $\mathbf{AF}$. A structural relaxation was then carried out in which this diffusing atom was constrained to remain in this plane, whereas all other atoms were allowed to move with no constraints imposed upon them. This is a far more general relaxation than that described in the previous paragraph as the diffusing atom can move off the [111] symmetry axis. This was repeated for a variety of fractional moves, α, and the energy determined as a function of α. The results are given in Table II for the neutral vacancy and Table III for the negative vacancy.

With reference to Figs. 7 and 8, an accurate picture of the diffusion path can be visualized. By symmetry, the total energies for the diffusing atom in each (111) plane between points E and F along the second half of the diffusion path should be the same as those for the first half (between A and E), which are calculated here. The highest energy position for the atom between atomic sites A and E is hence the energy barrier for diffusion. We find that this point does in fact occur for $\alpha = 0.5$, but at this saddle point the diffusing atom is 0.4 Å off the [111] axis for both charge states. In this way, the

TABLE II. The energy change associated with the diffusion of a neutral vacancy. This is given as a function of α, which is defined in the text. Also given are the off-axis displacement vector (d_x, d_y, d_z) and its magnitude, d. The energy is given in eV and is relative to the energy of a relaxed neutral vacancy.

α	Energy (eV)	d_x (Å)	d_y (Å)	d_z (Å)	d (Å)
0.00	0.00	0.00	0.00	0.00	0.00
0.13	0.29	0.07	−0.04	−0.04	0.09
0.21	0.83	0.12	−0.06	−0.06	0.15
0.27	1.27	0.20	−0.10	−0.10	0.18
0.33	1.68	0.27	−0.13	−0.13	0.24
0.39	2.09	0.31	−0.16	−0.16	0.38
0.41	2.30	0.32	−0.16	−0.16	0.39
0.44	2.50	0.32	−0.16	−0.16	0.39
0.47	2.67	0.32	−0.16	−0.16	0.39
0.48	2.74	0.31	−0.16	−0.15	0.38
0.50	2.80	0.22	−0.29	0.07	0.37

TABLE III. The energy change associated with the diffusion of a negative vacancy. This is given as a function of α, which is defined in the text. Also given are the off-axis displacement vector (d_x, d_y, d_z) and its magnitude. The energy is given in eV and is relative to the energy of a relaxed negative vacancy.

α	Energy (eV)	d_x (Å)	d_y (Å)	d_z (Å)	d (Å)
0.00	0.00	0.00	0.00	0.00	0.00
0.12	0.29	0.07	-0.03	-0.03	0.08
0.21	0.80	0.08	-0.04	-0.04	0.10
0.27	1.21	0.13	-0.07	-0.07	0.16
0.33	1.57	0.27	-0.13	-0.13	0.32
0.38	1.85	0.31	-0.16	-0.16	0.38
0.41	2.00	0.32	-0.16	-0.16	0.39
0.44	2.16	0.32	-0.16	-0.16	0.39
0.47	2.33	0.31	-0.16	-0.15	0.39
0.48	2.40	0.31	-0.16	-0.16	0.38
0.50	2.47	0.24	-0.27	0.03	0.36

diffusion energy was found to be 2.8 eV for the neutral vacancy and 2.5 eV for the −1 vacancy.

The position of the diffusing atom can be written as the sum of two vectors, one being $\alpha\mathbf{R}_A + (1-\alpha)\mathbf{R}_F$, the movement of the atom along the [111] direction, and the other being the perpendicular displacement of the atom off the symmetry axis. As can be seen from Tables II and III, the displacement is almost exactly along [2$\bar{1}\bar{1}$] for $0 \leq \alpha \leq 0.45$. For values of α between 0.45 and 0.55, the diffusing atom rotates around the [111] symmetry axis by 60°.

This diffusion path can be understood by considering the chemical bonding present. As the diffusing atom moves between points A and E it remains closest to, and equidistant from, atoms B and C until it is within 0.05 Å of the midpoint. By doing this only one bond, to atom D, is significantly lengthened, whereas atoms B and C move in such a way as to maintain a reasonable bond-length between themselves and the diffusing atom. This movement reduces the energy cost of this displacement. The path taken for $0.45 \leq \alpha \leq 0.55$ is governed by the need for the diffusing atom to move through 60° in the (111) plane in order to follow a path to atomic site F, while being again closest to, and equidistant from, two atoms. With reference to Fig. 8, if initially the atom traveled between points A and E with atoms B and C most closely bonded to it for most of the distance, then between points E and F it would move so that it was closest to either atoms I and G or atoms I and H. There are three equivalent diffusion paths on either side of the midpoint, each remaining closest to a different pair of atoms. These neighboring atoms, of course, undergo large displacements. Atoms B and C move in the same direction as the diffusing atom, while atom D relaxes back towards the three atoms it is still attached to, changing its bonding towards the favored sp^2, giving an additional gain of energy.

Finally, spin-polarized calculations were carried out for the end-point and saddle-point of negative vacancy dif-

fusion. The use of the local-spin-density approximation is necessary to correctly model this charge state of the vacancy. All other details of the calculation were as for the spin-averaged work described above. The end-point calculation was performed with spin $S = \frac{3}{2}$, which is accepted as the spin state of the ground state of the negative vacancy (which was also verified in Sec. IV B). The saddle point was assumed to be in the plane midway between the two atomic sites, as was found for both charge states in the spin averaged case. Two saddle point calculations were carried out with spin $S = \frac{3}{2}$ and $S = \frac{1}{2}$. The barrier energies were thereby found to be 3.4 eV for the $S = \frac{1}{2}$ case and 4.3 eV for the $S = \frac{3}{2}$ case. At the saddle point the diffusing atom is displaced off the [111] axis by 0.3 Å in both spin states.

The diffusion energy found for the neutral vacancy can be compared favorably with the experimental value of 2.3 ± 0.3 eV.[17] This experimental value was attributed to the diffusion of the neutral vacancy, and it was deduced that the diffusion energy of the neutral vacancy is less than that of the negative vacancy. Our result agrees with this conclusion, and disagrees qualitatively with the theoretical result[3] that found the vacancy diffusion energy to be 1.7–1.9 eV with the lower energies for the higher charge states and the highest for the tetrahedral neutral vacancy.

Palmer[32] found two activation energies for diffusion in type IIa diamond at 1.62 eV and 2.35 eV. The lower value is very close to our value for self-interstitial diffusion and the higher value is in reasonable agreement with our lowest value for vacancy diffusion.

VII. CONCLUSIONS

We have performed *ab initio* calculations to study possible structures for an interstitial carbon atom in the diamond lattice and find that the ⟨100⟩ split interstitial defect structure is the only stable configuration for an interstitial atom in the neutral, −1, +1, and +2 charge states. This defect has symmetry D_{2d} and gives rise to two degenerate one-electron energy levels of symmetry e in the band gap, into which two electrons are placed. We find the ground state of this structure to be $^1B_1$. However, a Jahn-Teller distortion is also possible in the neutral or singly charged states, which splits the two one-electron states and reduces the symmetry to D_2. The energy gain from this distortion is 0.6 eV. To our knowledge this effect has never previously been reported. The highest-frequency vibrational mode of this defect was deduced to be an infrared inactive A_1 mode at 2023 cm^{-1}, with two active modes of B symmetry at 1590 and 1600 cm^{-1}. These modes drop to 1984 cm^{-1}, 1560 cm^{-1}, and 1595 cm^{-1} if one of the central atoms is a ^{13}C atom and to 1944 cm^{-1}, 1557 cm^{-1}, and 1564 cm^{-1} if both of the central atoms are ^{13}C atoms. We find the migration energy of this defect to be 1.7 eV. Interstitial atoms in the hexagonal, tetrahedral, bond-centered, and ⟨110⟩ split interstitial structures all move to form ⟨100⟩ split interstitial defect structures when the atoms are relaxed.

We have studied the vacancy in diamond in the neutral and −1 charge states. For the neutral vacancy, we find

the four atoms surrounding the vacancy relax outwards from their positions in the perfect lattice structure by 0.2 Å, a different conclusion to previous work. This defect can also undergo a Jahn-Teller relaxation, which reduces the symmetry from T_d to D_{2d}. For optical experiments carried out at room temperature, this is a dynamic effect. The Jahn-Teller energy was calculated to be 0.36 eV, and the migration energy 2.8 eV.

For the negatively charged vacancy, we find the ground state to be $^4A_2$ in agreement with experiment. A well known signature of this defect is the ND1 optical absorption at 3.149 eV, which is believed to occur between the ground state and an excited state $^4T_1$. We find the energy of this transition to be 3.3 eV, supporting this assignment. The atomic structure of this ground state retains the T_d symmetry of the lattice and the four atoms surrounding the vacancy relax outwards by 0.2 Å. Clearly a Jahn-Teller distortion of this defect is possible. We find that the lowest energy distorted structure, which has $S = \frac{1}{2}$ and C_{3v} symmetry, has an energy 0.24 eV *higher* than the undistorted structure, showing the dominance of many-body effects over the energy gain from structural relaxation. We obtain 3.4 eV for the migration energy of this defect in its ground state. Finally, we calculate the formation energy for a vacancy-$\langle 100 \rangle$ split interstitial pair to be 20 eV.

ACKNOWLEDGMENTS

[1] C. Weigel, D. Peak, J. W. Corbett, G. D. Watkins, and R. P. Messmer, Phys. Rev. B **8**, 2906 (1973).

[2] A. Mainwood, F. P. Larkins, and A. M. Stoneham, Solid-State Electron. **21**, 1431 (1978).

[3] J. Bernholc, A. Antonelli, T. M. Del Sole, Y. Bar-Yam, and S. T. Pantelides, Phys. Rev. B **61**, 2689 (1988).

[4] D. J. Chadi, Phys. Rev. B **46**, 9400 (1992).

[5] G. Davies, J. Phys. C **14**, L391 (1981).

[6] G. Davies, J. Phys. C **15**, L149 (1982).

[7] G. Davies, Proc. R. Soc. London **338**, 359 (1974).

[8] C. D. Clark and E. W. J. Mitchell, *Conference on Radiation Damage in Semiconductors* (Gordon and Breach, New York, 1970).

[9] G. Davies, Nature **269**, 498 (1977).

[10] J. Isoya *et al.*, Phys. Rev. B **45**, 1436 (1992).

[11] J. C. Bourgoin and B. Massarani, Phys. Rev. B **14**, 3690 (1976).

[12] C. D. Clark, P. Kemmey, and E. W. J. Mitchell, Discuss. Faraday Soc. **31**, 96 (1961).

[13] W. Kohn, Phys. Rev. **94**, 1409 (1954).

[14] R. Baüerlein, Z. Naturforsch. Teil A **14**, 1069 (1959).

[15] R. Baüerlein, Z. Phys. **176**, 498 (1963).

[16] R. Baüerlein, in *Proceedings of the International School of Physics "Enrico Fermi"* (Academic, New York, 1962), p. 358.

[17] G. Davies, S. C. Lawson, A. T. Collins, A. Mainwood, and S. J. Sharp, Phys. Rev. B **46**, 13 157 (1992).

[18] S. C. Lawson, G. Davies, A. T. Collins, and A. Mainwood, J. Phys. Condens. Matter **4**, L125 (1992).

[19] W. Kohn and L. J. Sham, Phys. Rev. **140**, A1133 (1965).

[20] G. B. Bachelet, D. R. Hamann, and M. Schluter, Phys. Rev. B **26**, 4199 (1982).

[21] R. Jones, J. Phys. C **21**, 5735 (1988).

[22] R. Jones and P. R. Briddon, S. Öberg, Philos. Mag. Lett. **66**, 67 (1991).

[23] P. R. Briddon and R. Jones, Physica B **185**, 179 (1993).

[24] U. von Barth, Phys. Rev. B **20**, 1693 (1979).

[25] A. Mainwood, J. Phys. C **11**, 2703 (1978).

[26] C. A. Coulson and M. J. Kearsley, Proc. R. Soc. London, Ser. A **241**, 433 (1957).

[27] J. E. Lowther, Phys. Rev. B **48**, 11 592 (1993).

[28] M. Lannoo and A. M. Stoneham, J. Phys. Chem. Solids **29**, 1987 (1968).

[29] J. E. Lowther and J. A. van Wyk, Phys. Rev. B **49**, 11 010 (1994).

[30] For example, G. D. Watkins, in *Deep Centers in Semiconductors*, edited by S. T. Pantiledes (Gordon and Breach, New York, 1986), p. 147.

[31] O. Sugino and A. Oshiyama, Phys. Rev. Lett. **68**, 1858 (1992).

[32] D. W. Palmer, Ph.D. thesis, University of Reading, 1961.